Study of Phase Separation in Interpenetrating Polymer Networks Using Nitroxide Spin Labels

Shulamith Schlick,* Raymond D. Harvey, M. G. Alonso-Amigo, and Daniel Klempner†

Department of Chemistry, University of Detroit, Detroit, Michigan 48221-9987.
Received February 26, 1988; Revised Manuscript Received July 18, 1988

ABSTRACT: The compatibility of the two components in semiinterpenetrating polymer networks (semi-IPNs) and the corresponding linear blends (LBs) is studied for the first time by using the nitroxide spin label method. The IPNs and LBs are composed of poly(vinyl chloride) (PVC) and a cross-linked polyurethane (PU) based on polycaprolactone glycol (PCL) and the aromatic isocyanate 4,4′-methylenebis(phenyl isocyanate) (MDI). The strategy adopted in this study is to incorporate spin-labeled PVC in the semi-IPNs and LBs. The temperature dependence of the ESR spectra from the label attached to PVC in blends with different ratios of PVC and PU was measured. ESR spectra from spin-labeled PVC indicate that the label is sensitive to the segmental motion above T_g; the activation energy for this motion is 17.4 kcal/mol. The spacial resolution of the label is 5–10 monomeric units of PVC. Polyurethane based on polycaprolactone glycol and MDI was spin labeled at the terminal isocyanate group; the ESR spectra show composite spectra, with fast and slow components. Two components were also detected in the ESR spectra from the IPNs and LBs. We suggest that the two phases in PU consist of crystalline PCL and amorphous PCL; the aromatic isocyanates are part of the amorphous phase. The ESR results obtained for the IPNs and LBs suggest that PVC partitions between the two phases in PU. The heterogeneity in the local environment of the label in IPNs and LBs is reflected in the line shapes of motionally averaged spectra detected around 400 K. These line shapes can be simulated by a distribution of g_{iso} and A_{iso} values. The existence of this distribution is supported by results from samples annealed at 400 K and by comparison of spectra from IPNs and LBs with those obtained for spin-labeled PVC. Qualitatively, the width of the distribution for each system, deduced from spectra simulation, is an indicator of the degree of mixing. The distribution is thought to arise from a range of local environments of the label, differing in their polarity. Hydrogen bonding between the methine hydrogen in PVC to the carbonyl group in PCL and hydrogen bonding between the N–O group of the label and the N–H group of the urethane might increase the local polarity compared with that in pure PVC and give rise to the assumed distribution widths δg and δA.

Introduction

Stable nitroxide radicals have been extensively used for the study of motional processes and phase transitions in polymers and copolymers,[1] in block polymers[2,3] and in polymer blends.[4] The principal values of the anisotropic molecular g tensor and of the electron–nuclear hyperfine interaction tensor from the nitrogen nucleus ($I = 1$) are affected by temperature variations in a way which depends on the motion in the medium being probed. Changes in the line shapes and in the separation between the outermost signals which appear in the ESR spectra of the probes are measured as a function of temperature. The temperature at which this separation is 50 G, or T_{50G}, has been correlated with the glass transition temperature T_g.[1] The difference between the values of T_g and T_{50G} has been used to deduce the ratio between the volumes of the probe and of the segment whose motion is responsible for the appearance of T_g;[5,6] this difference seems to depend on whether the nitroxide reporter molecule is mixed with the polymer (a "probe") or covalently linked to the polymer (a "label").

In some cases ESR spectra of the probe can also reflect different environments in a given sample, with different rates of motion; "fast" and "slow" components are detected and they refer to the appearance of isotropic spectra due to fast motion and of anisotropic spectra for immobilized probes or for slower motions. The partition of the spin probe or label and the detection of a composite ESR spectrum indicates a heterogeneous medium; in polymer language this usually means a complex morphology and phase separation, both of which are common occurrences in polymer mixtures.

Interpenetrating polymer network (IPNs) are polymer blends obtained by simultaneous or sequential cross-linking of two polymers. Semi-IPNs are obtained by cross-linking one type of chain in the presence of a linear polymer. It is believed that these procedures increase the degree of mixing of the two components or at least decrease the rate of phase separation. Measurement of T_g is a useful method for the study of morphologies in IPNs and semi-IPNs. The correlation between this macroscopic property and the phase structure on a molecular level is, however, at best uncertain. The major objective in our studies of polymer blends in general and more specifically in IPNs is to develop methods for the study of the degree of mixing in the IPNs on a molecular scale.

In this report we describe the application of this method to the study of compatibility of two components in semi-IPNs composed of polyvinyl chloride (PVC) and a cross-linked polyurethane (PU) based on polycaprolactone glycol (PCL); the corresponding linear blends (LBs) are also studied, for comparison. The strategy adopted in this study is to prepare PVC labeled with a nitroxide group and then incorporate it in the IPNs and LBs; the temperature dependence of the ESR spectra from the label attached to the PVC backbone in blends with different ratios of PVC and PU was measured. Any changes in the ESR spectra of the label in the IPNs and LBs compared to pure PVC are thus due to polymer mixing.

Several reasons determined our choice of the components in the semi-IPN. First, the morphologies of the major constituent polymers, PVC and PCL, are fairly well understood. The glass transition temperature of PVC is 356 ± 10 K, depending upon the method of polymerization; a broad transition below T_g has also been detected.[7,8] PCL has a glass transition temperature of 202 K in the amorphous material and 218 K in the semicrystalline

† Polymer Technologies, Inc., Detroit, MI 48221-9987.

0024-9297/89/2222-0822$01.50/0

polymer;[9,10] its melting point is about 330 K. Second, blends of PVC and PCL have been extensively studied by a variety of methods.[11-15] The results obtained indicate that compatible blends are obtained for compositions that contain up to 60% PVC. There is evidence that enrichment of the blend in PVC reduces the degree of crystallinity of PCL and a recent nuclear magnetic resonance (NMR) study has specifically focused on blends containing 70% or more of PVC, in order to avoid contributions from the crystalline phase of PCL.[14]

Third, the phase structure in bulk hard-segment polyurethanes based on aromatic isocyanates and in segmented PU containing PCL has also been studied, using NMR,[15] dielectric relaxation,[16] differential scanning calorimetry (DSC),[17] Fourier-transform infrared (FTIR) spectroscopy,[18] and small-angle X-ray diffraction.[19] Fourth, the phase structure in blends of PCL-based PU with PVC has been studied by X-ray diffraction and electron microscopy;[20] the results indicate that in these blends the compatibility is reduced, compared with that in PVC/PCL blends, due to the presence of the aromatic isocyanates. Finally, the macroscopic phase structure in the IPNs investigated in this report has also been studied by dynamical mechanical methods.[21]

To the best of our knowledge this is the first application of the nitroxide spin label method to an IPN system.

Some initial results have been reported.[22]

Experimental Section

Spin-Labeled PVC. PVC (Borden, MW 58000) was purified by dissolution in tetrahydrofuran (THF), precipitation by methanol, and vacuum drying. The labeling of the PVC was done by mixing 100 mL of a 2.3% by weight solution of PVC in THF with 100 mL of a methanol solution containing sodium methoxide and the spin probe 4-hydroxy-2,2,6,6-tetramethylpiperidinyl-1-oxy (tempol, from Aldrich). The mixture was stirred for 6 h and the precipitate, which included the labeled PVC, was reprecipitated from methanol and dried in vacuum for 24 h. The amount of sodium methoxide is the factor controlling the concentration of the spin label in PVC. The amount of label in the preparation was reduced until no effect on the ESR line widths was detected. The notation for this sample is PVC-L.

Spin-Labeled Semi-IPNs. The prepolymer mixture in THF was prepared by the usual methods from 4,4'-methylenebis(phenyl isocyanate) (MDI, from Mobay) and PCL (Union Carbide, MW 2000) in a molar ratio 3/2. To this solution, a 10% solution of spin-labeled PVC was added, together with triethanolamine (TEA, from Matheson) as the cross-linking agent and several drops of dibutyltin dilaurate (T-12, from M & T Chemicals) as the catalyst. The amount of TEA was 1.8 wt% of the combined weights of PCL and MDI. The curing was done at 343 K in vacuum for 24 h. Additional experimental details have been published.[23] Four IPN samples have been prepared, with PU/PVC ratios of 30/70, 40/60, 60/40, and 70/30. The notation used for these samples is IPN30, IPN40, IPN60, and IPN70.

Linear blends based on the same compositions were also prepared, using 1,4-butanediol instead of TEA. Curing was done at 333 K in vacuum for 1 h. The notation for these samples is LB30, LB40, LB60, and LB70.

Spin-labeled PU was prepared by following the same procedure as for the preparation of the semi-IPNs, except that a solution of tempol in THF was added instead of the PVC solution. The curing was done at 333 K for 1 h. The notation for this sample is PU-L.

Glass transition temperatures T_g based on the loss factor were obtained with a Rheovibron Dynamic Viscoelastometer (Model DDV-II-c, Toyo Baldwin Co., Tokyo).

ESR spectra were measured at X-band with a Bruker 200D SRC spectrometer operating at 9.7 GHz, with 100-KHz modulation. Spectra were measured in the temperature range 100–450 K by using the Bruker variable-temperature unit ER 4111 VT. ESR spectra at 77 K were measured in a finger Dewar inserted in the ESR cavity. The absolute value of the magnetic field was measured by using the Bruker ER 035M gaussmeter. Calibration of g values is based on DPPH (g = 2.0036) and Cr(III) in a single crystal of MgO (g = 1.9800). ESR spectra were calculated by using a Burroughs 6800 mainframe computer and plotted by an IBM PC and a Hewlett-Packard digital plotter.

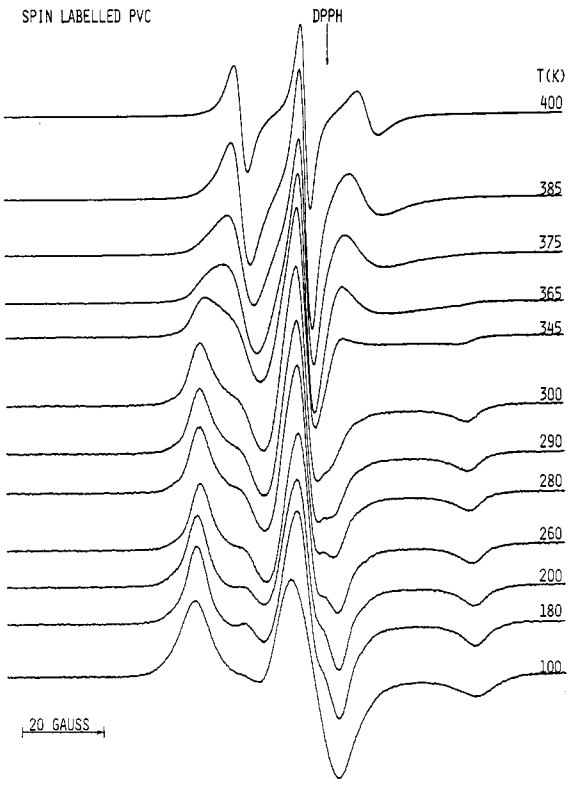

Figure 1. X-band ESR spectra of spin-labeled PVC in the temperature range 100–400 K.

Results

Spin-Labeled PVC. In this section we will analyze in detail the ESR spectra from spin-labeled PVC in order to deduce the energetics of the motion, the relation of the ESR spectra to the glass transition temperature T_g measured by other methods, and the size of the polymer segment involved in the motion corresponding to the glass transition. Because PVC is a component in all IPNs and LBs studied, this information is needed in order to assess the spacial sensitivity of the label.

ESR spectra of spin labeled PVC in the temperature range 100–400 K are shown in Figure 1; the spectrum at 77 K is identical with that at 100 K. Spectra were also taken above 400 K, up to 450 K; the only changes were in the line widths of the three isotropic lines, which become narrower at higher temperatures. At 450 K the amplitudes of the three lines are practically the same.

The temperature dependence of the spectra is due to the change in the motional correlation times τ_c. The two motional regimes usually detected in nitroxides correspond to the "rigid" spectra, with correlation times in the range of 10^{-7} to 10^{-9} s and "averaged", or isotropic, spectra with correlation times in the range 10^{-9} to 10^{-11} s. In Figure 1 these regions seem to be below and above 365 K, respectively. From the temperature variation of the separation between the two outermost lines of the ^{14}N hyperfine splitting (extreme separation, or $2A_{zz}$) we deduce that T_{50G} = 366 K and is identical, within ±1 K, with the glass transition temperature we measured by mechanical relaxation.

The best method to calculate the correlation times is by spectral simulations. By comparing the calculated spectra with experimental results, an empirical method for cal-

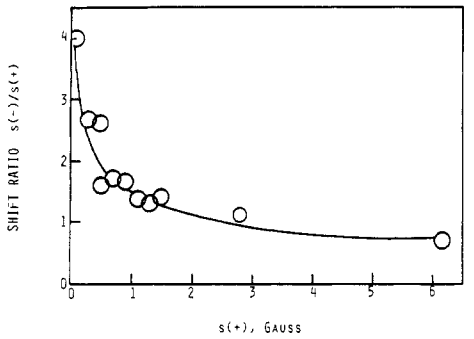

Figure 2. Shift ratio $s(-)/s(+)$ as a function of $s(+)$ for spin-labeled PVC. $s(+)$ and $s(-)$ are the shifts of the low-field and high-field line which define the extreme separation, from the position in the rigid limit at 100 K.

culating the correlation times for the low-temperature regime has been suggested; this method is based on the change in the value of $2A_{zz}$ with temperature, using eq 1.[24,25] In eq 1, $S = 2A'_{zz}/2A_{zz}$, where $2A_{zz}$ is the extreme

$$\tau_c = a(1 - S)^b \quad (1)$$

separation in the rigid limit and $2A'_{zz}$ is the separation at temperature T. The parameters a and b depend on the motional model and on the intrinsic line width. The choice of a and b can be facilitated by measuring the shifts of the low- and high-field lines, $s(+)$ and $s(-)$, respectively, in gauss, from their position in the rigid limit and plotting $s(-)/s(+)$ versus $s(+)$. For PVC such a plot is shown in Figure 2; the shape of the curve seems to suggest a Brownian diffusion mechanism.[26] For this motional model and an intrinsic line width of 3 G, the suggested values of a and b are $a = 5.4 \times 10^{-10}$ s and $b = -1.36$.[26] The choice of the line width is based on simulation of the rigid limit ESR spectrum from the labeled polymer at 100 K.

The correlation times in the high-temperature regime can be calculated from eq 2.[27]

$$\tau_c = 6.15 \times 10^{-10} H(0)\{R(+) + R(-) - 2\} \quad (2)$$

In eq 2, $R(\pm) = \Delta H(\pm)/\Delta H(0)$ where $\Delta H(+)$, $\Delta H(0)$, and $\Delta H(-1)$ are the line widths of the low field, center field, and high field, respectively; the numerical factor in eq 2 arises from $g_{iso} = 2.0059$, $A_{zz} = 34.6$ G, and $A_{iso} = 15.4$ G and by assuming that the hyperfine tensor of the nitroxide radical is axial.

An Arrhenius plot of ln τ_c versus $1/T$ in the entire temperature range measured for PVC is shown in Figure 3. Two very clear motional regimes are evident and the boundary is at ca. 370 K, close to the T_{50G} temperature of 366 K. From Figure 3 we deduce the activation energies and preexponential factors in the two regimes: At low temperature $E_{act} = 2.0$ kcal/mol and $\tau_0 = 8 \times 10^{-10}$ s. At high temperature $E_{act} = 17.4$ kcal/mol and $\tau_0 = 8 \times 10^{-19}$ s.

ESR spectra of PVC containing various probes have been measured before.[28-30] To the best of our knowledge this is the first study of spin-labeled PVC. The activation energy obtained in this study for the low-temperature range is similar to that obtained for the tempo *probe* in PVC,[30] 2.0 and 2.1 kcal/mol, respectively, but significantly lower than the value of 14 kcal/mol obtained by dielectric and mechanical relaxation.[30] It has been suggested that the low-temperature region motion is due to the local motion of the nitroxide radical in a structural defect similar in size; this explains the fact that the activation energy is around 2 kcal/mol for tempo and other nitroxide probes in different amorphous polymers.[29,31] The results obtained for the *label* in this study seem to support this description.

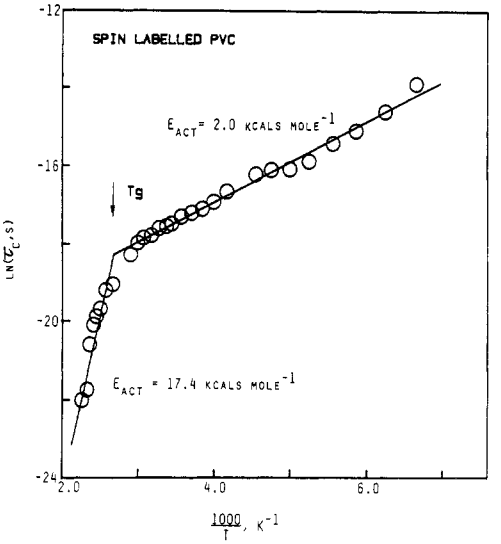

Figure 3. Variation of the correlation time τ_c with T^{-1}, for spin-labeled PVC. The straight lines are best fits to the experimental points in the low-temperature regime (below 370 K) and in the high-temperature regime (above 370 K).

It is significant that the activation energy measured at high temperatures is larger for the label than for the probe, 17.4 kcal/mol versus 10 kcal/mol. The preexponential factor we deduced, 8×10^{-19} s, is too high for a thermally activated process, indicating that this type of data treatment is only an approximation; the segmental motion around T_g is a function not only of the temperature but also of the partial free volume in the polymer.[32]

The fundamental questions which needs to be addressed in this study is what is the spacial resolution of the label or, in other words, what is the region which we can examine by spin-labeled PVC. While the low-temperature data seem to suggest that the label "sits" at a defect site and is rather insensitive to the specific location, the high-temperature region seems to reflect the glass transition temperature, because we found that $T_{50G} = T_g$. We can therefore assume that the label is part of the polymer segment whose motion is activated at T_g and thus the label explores a space which is roughly equal to this polymer segment. Based on the free volume treatment of Bueche, Kusumoto et al. suggested eq 3 for calculating the ratio

$$T_{50G} - T_g = 52[2.9f(1 - \ln f) - 1] \quad (3)$$

f, with $f = V(\text{label})/V(\text{segment})$.[5] For spin-labeled PVC, $T_g = T_{50G}$ and we obtain $f = 0.1$. The volume of the label is 170 Å^3.[5] This result indicates that the volume of the motional segment is ca. 1700 Å^3. The volume of one monomer unit is ca. 160 Å^3, so we obtain that about 10 monomer units are involved in the segmental motion above T_g.

A refinement of the Kusumoto approach leads to eq 4.[6]

$$\ln \tau_c = \ln \tau_0 + f[2.3c_{1g}c_{2g}/(T - T_g + c_{2g})] \quad (4)$$

In this equation, c_{1g} and c_{2g} are the WLF (Williams, Landel, Ferry[32]) "universal" parameters equal to 17.44 and 51.6, respectively, and f is defined as before. The plot of ln τ_c above T_g versus $[2.3c_{1g}c_{2g}/(T - T_g + c_{2g})]$ is shown in Figure 4; the reasonably linear plot gives a slope of $f = 0.198$. The result implies that the polymer segment undergoing segmental motion above T_g is about the size of five monomeric units. The two approaches therefore suggest that the region explored by the label is of the order of 5–10 monomeric units of PVC.

IPNs and LBs Containing Spin-Labeled PVC. ESR spectra of IPN30, IPN40, IPN60, and IPN70 in the tem-

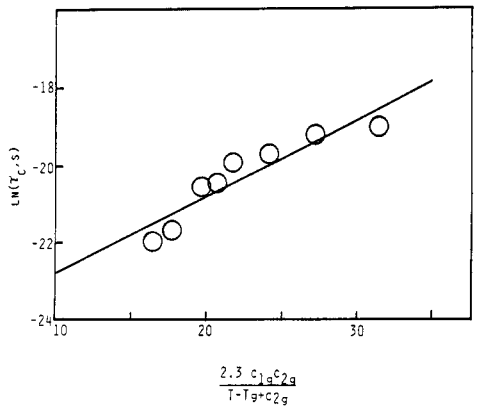

Figure 4. Plot of τ_c versus $2.3c_{1g}c_{2g}/(T - T_g + c_{2g})$ (eq 4).

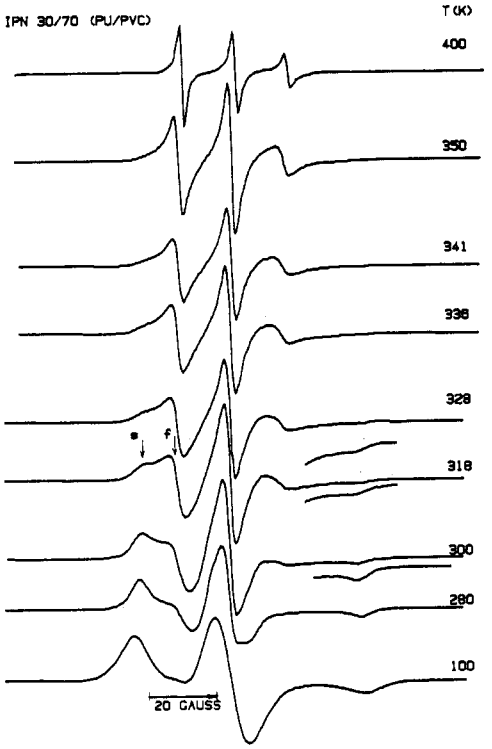

Figure 5. X-band ESR spectra of spin-labeled PVC in IPN30 as a function of T. At 318 K the low-field "slow" and "fast" components are indicated by "s" and "f", respectively.

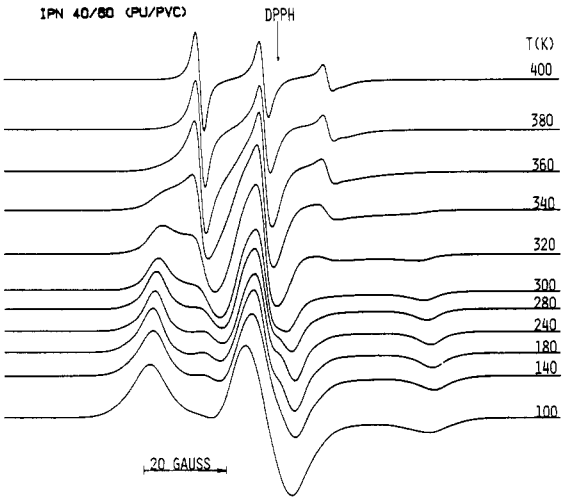

Figure 6. X-band ESR spectra of spin-labeled PVC in IPN40 as a function of T.

perature range 100–420 K are presented in Figure 5–8. ESR spectra from the corresponding linear blends, samples

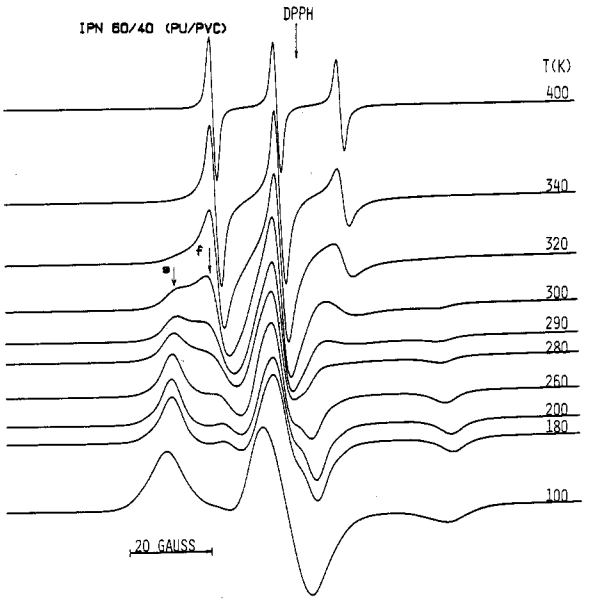

Figure 7. X-band ESR spectra of spin-labeled PVC in IPN60 as a function of T. At 300 K the low-field "slow" and "fast" components are indicated by "s" and "f", respectively.

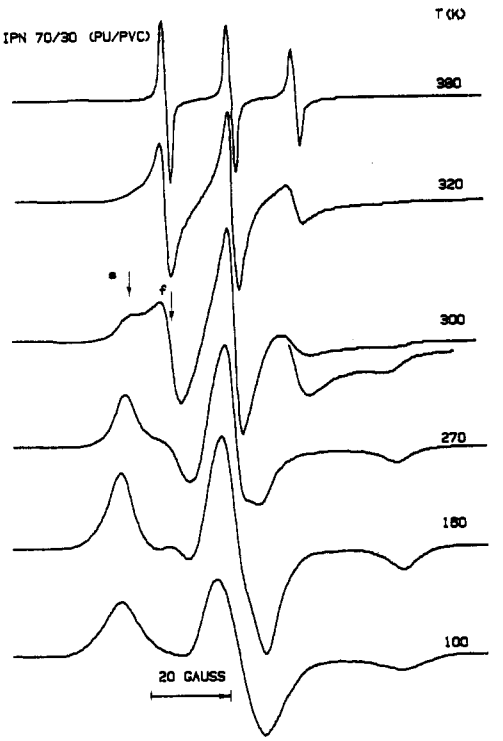

Figure 8. X-band ESR spectra of spin-labeled PVC in IPN70 as a function of T. At 300 K the low-field "slow" and "fast" components are indicated by "s" and "f", respectively.

LB30, LB40, LB60, and LB70, are shown in Figures 9–12, in the same temperature range. Above 420 K the signals disappear rapidly and irreversibly; this behavior is in contrast with the stability of the label in pure PVC, where spectra were measured up to 450 K, with no measurable decrease in the signal intensity.

Two significant differences can be noted between the spectra shown in Figures 5–12, compared to the results presented for pure PVC in Figure 1. First, two clear components are visible in all spectra shown in Figures 5–12 in the temperature range 280–320 K, indicating a partition of the spin-labeled PVC into two environments with different mobilities. In some figures the two components at low field are indicated by "s" (slow) and "f" (fast). The

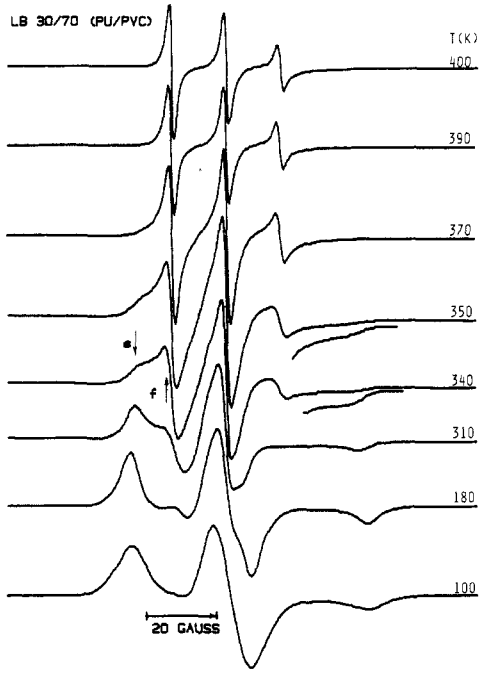

Figure 9. X-band ESR spectra of spin-labeled PVC in LB30 as a function of T. At 340 K the low-field "slow" and "fast" components are indicated by "s" and "f", respectively.

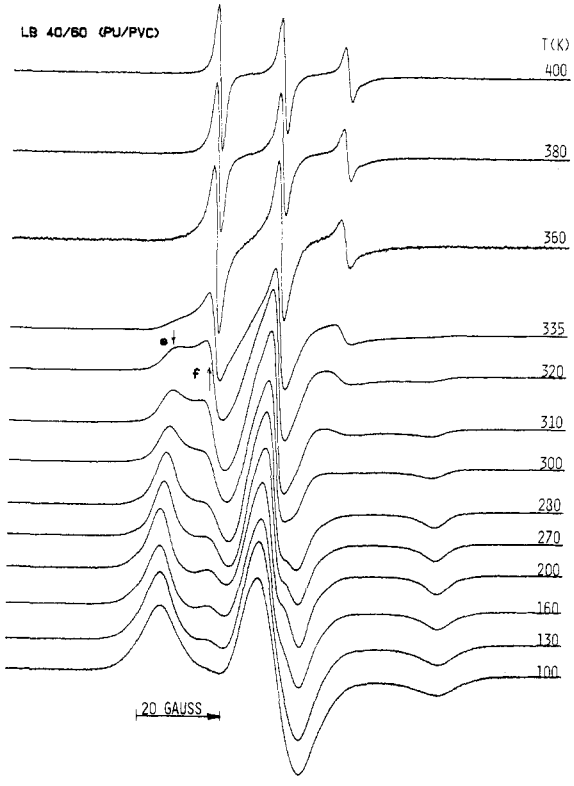

Figure 10. X-band ESR spectra of spin-labeled PVC in LB40 as a function of T. At 320 K the low-field "slow" and "fast" components are indicated by "s" and "f", respectively.

lowest temperatures which enable detection of an isotropic component (from the "fast" component) in the series of spectra shown in Figures 5–12 are given in Table I. The temperatures are accurate to about ±7 K. The T_{50G} temperatures, corresponding to the "slow" component, are also given in Table I. Second, in all samples at high temperature (around 400 K) the IPNs and LBs shown a gradual decrease in amplitude, from low to high field, and the narrowest line is the low field line. For pure PVC the center line is the narrowest at high temperatures. These

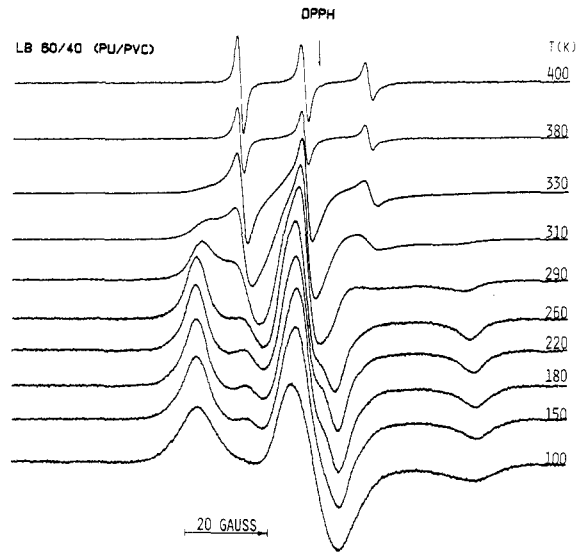

Figure 11. X-band ESR spectra of spin-labeled PVC in LB60 as a function of T.

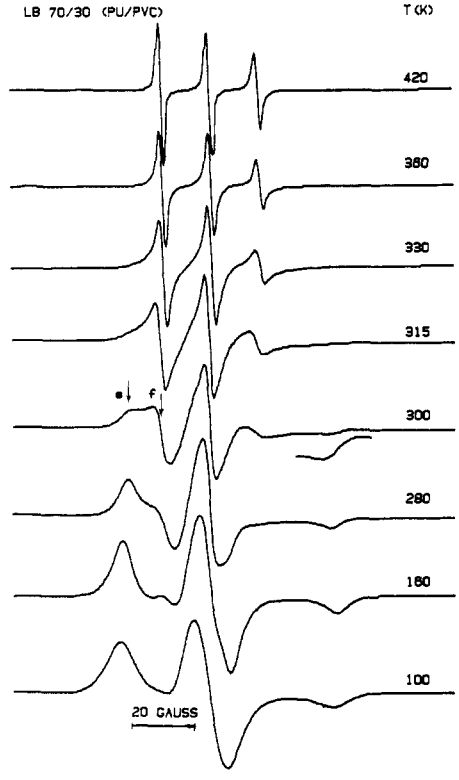

Figure 12. X-band ESR spectra of spin-labeled PVC in LB70 as a function of T. At 300 K the low-field "slow" and "fast" components are indicated by "s" and "f", respectively.

line shapes can be quantified by the amplitude ratios $r(0) = h(0)/h(+)$ and $r(-) = h(-)/h(+)$, where $h(+)$, $h(0)$, and $h(-)$ are the amplitudes (heights) of the low-field, center-field, and high-field signals, respectively. These ratios are collected in Table I.

Annealing of the IPNs at 400 K for 30–45 min results in significant changes in the ESR spectra at 400 K, without affecting the spectra at lower temperatures. More specifically, the amplitude ratios $r(0)$ and $r(-)$ are closer to 1 in these annealed samples. In Figure 13 we compare the ESR spectra at 400 K for IPN40 and IPN60 before and after annealing. The change in the amplitude ratios is largest in these samples, as also indicated in Table I. No significant changes have been detected for the LBs on annealing.

Table I

sample	T_{50G}, K[a]	T_{iso}, K[b]	$h(-)/h(+)$[c] before anneal	$h(-)/h(+)$[c] after anneal	$h(0)/h(+)$[d] before anneal	$h(0)/h(+)$[d] after anneal	$\delta g \times 10^4$[e]	δA, G[e]
PVC-L	366		same		same			
PU-L	308	285	0.49	0.57	0.85	0.86	5.0	1.0
IPN30	347	310	0.34	0.36	0.81	0.85	6.0 (5.8)	1.5 (1.5)
IPN40	352	320	0.27	0.51	0.76	0.88	6.8 (4.4)	1.5 (1.0)
IPN60	331	300	0.51	0.73	0.85	0.95	4.6 (3.0)	1.0 (0.6)
IPN70	321	290	0.47	0.56	0.81	0.86	5.2 (4.4)	1.0 (0.8)
LB30	360	325	0.35	0.36	0.82	0.83	6.0	1.5
LB40	340	310	0.40	0.38	0.79	0.79	6.0	1.2
LB60	332	300	0.41	0.41	0.78	0.78	6.0	1.2
LB70	326	295	0.44	0.45	0.81	0.82	5.8	1.2

[a] Corresponds to the "slow" component in a composite spectrum. The accuracy is ±3 K. [b] This is the lowest temperature corresponding to the appearance of a motionally averaged "fast" component in a composite spectrum. The accuracy is ±7 K. [c] This is the amplitude ratio of the center-field line to the low-field line at 400 K. [d] This is the amplitude ratio of the high-field line to the low-field line at 400 K. [e] Obtained by calculating spectra with $\Delta H^R = 1$ G. The parameters in parantheses are for the annealed samples. For the LBs, annealing does not change the line shapes and therefore the distribution parameters are not affected.

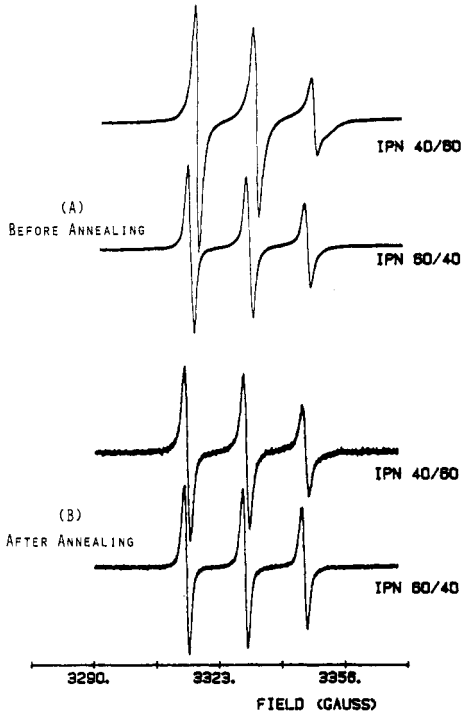

Figure 13. Change in the X-band ESR spectra of IPN40 and IPN60 at 400 K due to annealing at 400 K for 15–20 min.

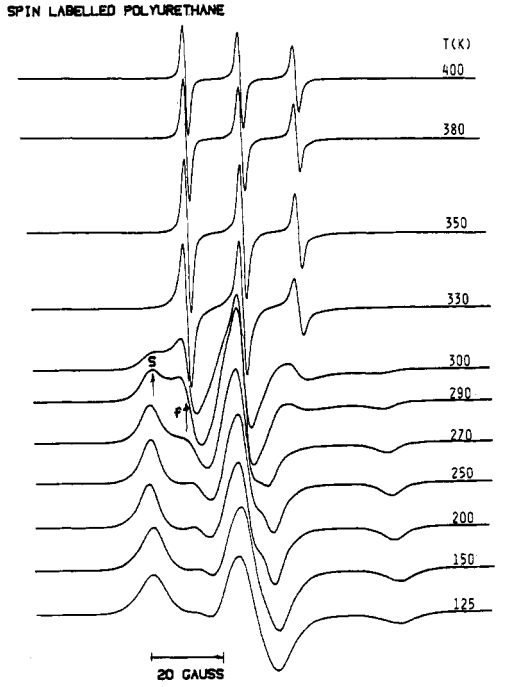

Figure 14. X-band ESR spectra of spin-labeled PU as a function T. At 290 K the low-field "slow" and "fast" components are indicated by "s" and "f", respectively.

Spin-Labeled PU. In order to better understand the molecular basis for the presence of two components in the IPNs and LBs, we measured the ESR spectra of spin-labeled PU. Because of the method of preparation, which involves the reaction between 4-hydroxy-tempo and a terminal NCO group in PU, the label is most likely located at the *end* of a polymer chain. ESR spectra for spin-labeled PU (PU-L) are shown in Figure 14. Clear partition of the label into two environments is detected; an isotropic component appears around 285 K and T_{50G} for the slow component is 308 K. The T_{50G} value for the slow component is very close to the melting point of 330 K for crystalline PCL; the temperature of 285 K for the appearance of the fast components is higher than the corresponding T_G of 208 K, most likely because the aromatic isocyanate is also part of the amorphous phase, as has been suggested before.[20]

It is also important to note that the line-shape pattern at high temperatures in PU-L is similar to that observed for the blends, is different from that observed in pure spin-labeled PVC and is not affected by annealing at 400 K.

The literature on spin labels in PU is limited and the results are extremely sensitive to the composition of the polymer, its degree of crystallinity, and the location of the label. In a PU prepared from MDI and poly(tetramethylene glycol), the label was located in the chain extender and the curing agent was trimethylolpropane.[33] For a high content of the hard segment, no evidence for motional averaging of the label was observed up to the highest temperature in these experiments, 410 K. For a lower content of the hard block, a T_{50G} value of 330 K was measured. In a more recent paper,[34] a diol nitroxide spin label was inserted in the hard segment; two environments of the label were observed, with T_{50G} values of 410 and 450 K. These values can be compared with our observation of an isotropic component at 285 K and a T_{50G} value of 308 K, indicating the rather broad range of results that can be obtained for different labels and label locations.

Discussion

Phase Separation in IPNs and LBs. All samples studied are *clear* and exhibit *one* glass transition temperature. By contrast, the results presented in Figures 1–12 and 14 indicate beyond reasonable doubt that the PU

used for the preparation of IPNs and LBs is phase separated and that this separation persists in the blends. It seems that different methods of measurement give different results. The spin-label method is sensitive to the *molecular* environment and provides information on a molecular scale.

The existence of two components in the ESR spectra of the IPNs and LBs can be explained by assuming that the labeled PVC forms blends with each of the two components existing in PU, giving the two environments detected in these systems. Support for this assumption is obtained by observing that the values of the T_{50G} for the slow component in IPNs and LBs, which range between 360 and 321 K, are intermediate between the T_{50G} value for PVC (366 K) and the slow component of PU (308 K). Similarly, the temperatures corresponding to the appearance of a fast component, which range between 320 and 290 K, are between the T_{50G} value for PVC and that of the fast component in PU (285 K), as shown in Table I.

The composition of each phase in the phase-separated IPNs and LBs could, in principle, be deduced from the total composition of the samples, the values of T_{50G} of each phase in the phase-separated samples, and the assumption that $T_{50G} = T_g$, so that the Fox equation can be used. The problem is, however, that it is hard to decide what exactly the T_{50G} values are for the "pure" components. It would be dangerous to use the transitions temperatures indicated for PU in Table I, because these temperatures depend upon the location of the label, as discussed above. This fundamental difficulty forces us to abandon this approach. Instead, we will deduce information on the different environments of the label by an analysis of the line widths at high temperature, typically around 400 K.

Environment of the Nitroxide Label in IPNs and LBs. In all spectra present at 400 K, except in pure PVC, the line width increases from low to high field, creating a pattern with decreasing heights of the three lines as the magnetic field increases. This type of spectra has been simulated before,[35] for an anisotropic motion of the spin label; this means that the motional averaging processes are strongly orientation dependent. In this case "orientation" is the direction of the rotation axis with respect to the directions of the principal values of the g and hyperfine tensors. The line shapes described above successfully simulated the line shapes in spin-labelled poly(methyl methacrylate) (PMMA).

We believe that this approach is not applicable in the systems we investigate here for two main reasons. First, this line shape is not observed in PVC, to which the label is covalently bound. Second, the results of the annealing experiments indicated that this line shape is sensitive to the morphology of the system and to the segmental motion and not the local anisotropy of the label.

In this study we present an alternative model which simulates extremely well the increase in line width as the magnetic field increases and, in addition, explains the changes in the line shapes due to sample annealing. The model is based on the assumption of distribution widths δg and δA in the values of g_{iso} and A_{iso}, respectively. This distribution is detected around 400 K, because at this temperature the line widths are narrow enough, due to motional averaging, to observe the effect of the distribution. As will be seen below, excellent agreement with experimental spectra is obtained, for distribution parameters of a magnitude that is very reasonable for a nitroxide label.

According to this model, the line width at half-maximum intensity, ΔH, is composed of the residual width ΔH^R and a contribution from the distribution δH, as shown in eq 5.

$$(\Delta H)^2 = (\Delta H^R)^2 + (\delta H)^2 \tag{5}$$

The width due to the distribution, δH, depends on the m_I value, on the microwave frequency ν, and on the distribution widths δg and δA, as shown below.[36]

$$(\delta H)^2 = (m_I \delta A)^2 + \left(\frac{h\nu}{g_{iso}^2 \beta}\delta g\right)^2 - \frac{2\epsilon m_I h\nu}{g_{iso}^2 \beta}\delta g \delta A \tag{6}$$

In eq 6, ϵ is a parameter that indicates the extent of correlation between δg and δA. If $\epsilon = 1$, these distributions are "perfectly correlated", in the sense that all labels have the same ratio $\delta A/\delta g$. This is the assumption used in our simulations. The last term in the expression for the line width in eq 6 depends on the microwave frequency and can be either positive or negative. Measurements at two microwave frequencies can prove conclusively the existence of the distributions. This method has been applied to the ESR study of paramagnetic transition metal complexes at X- and S-bands.[36,37] It was not possible for us to measure ESR spectra at 400 K at a microwave frequency different from X-band.

In this study ESR spectra were calculated by using a code based on the program of Kasai,[38] modified in our laboratory to include the effect of the g_{iso} and A_{iso} distributions. The line widths are calculated from eq 5 and 6, and the spectra are obtained for Lorentzian line shapes for different values of the residual line width ΔH^R, for different values of the distribution widths δg and δA, and with $\epsilon = 1$.

The parameters used in calculating the ESR spectra are as follows: $g_{iso} = 2.0059$, $A_{iso} = 15.6$ G, and $\Delta H^R = 1$ G; δg is in the range 0.00–0.0020 and δA is in the range 0.0–1.5 G. Typical spectra for $\delta A = 1$ G and δg values of 0.0000, 0.0004, 0.0008, 0.0012, and 0.0018 are shown in Figure 15. It should be noted that for low values of δg, the central line has the highest amplitude and the smallest line width, irrespective of the value of δA; this is because A has zero contribution to the line width of the center line for which $m_I = 0$.

In Figure 16 we present the amplitude ratios $r(0)$ and $r(-)$ as a function of δg, for $\delta A = 0.3$, 0.4, 0.5, 0.6, 0.8, 1.0, and 1.5 G. The calculated amplitude ratios can be compared with the experimental values given in Table I. The range of experimental amplitude ratios can be simulated for δg values in the range 0.0002–0.0007 and δA values in the range 0.6–1.5 G; these values seems to be very reasonable for nitroxide labels.[39] The combinations of δg and δA that simulate the experimental results for each sample can be read directly from Figure 15 and are also given in Table I. The amplitude ratios for the annealed samples and the corresponding combination of δg and δA values that reproduce these ratios are also given in Table I.

The existence of a distribution of g_{iso} and A_{iso} values can arise from the presence of the label in environments of different polarities.[40,41] It is well-known that in more polar media the ^{14}N isotropic hyperfine splitting is larger and the isotropic g value is smaller than in nonpolar media.[40] For instance, the variation in A_{iso} is ca. 2.4 G and in g_{iso} it is 0.0005 when the solvent changes from a polar aqueous solution of 10 M LiCl to hexane; the large A_{iso} is correlated with a small g_{iso}. It has also been mentioned that a high value of A_{iso} is measured in solvents that are hydrogen bond forming.[42]

It has been suggested that the compatibility between PVC and PCL is due to hydrogen bonding between the methine hydrogen in PVC and the carbonyl group in

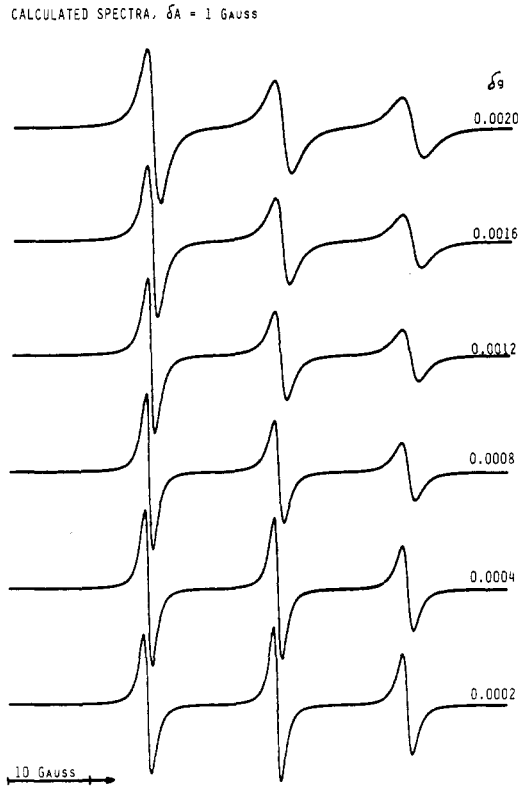

Figure 15. Calculated X-band ESR spectra of a nitroxide radical for δA = 1 G as a function of δg. The parameters used to calculate the spectra are as follows: g_{iso} = 2.0059, A_{iso} = 15.6 G, ϵ = 1, and ΔH^R = 1 G.

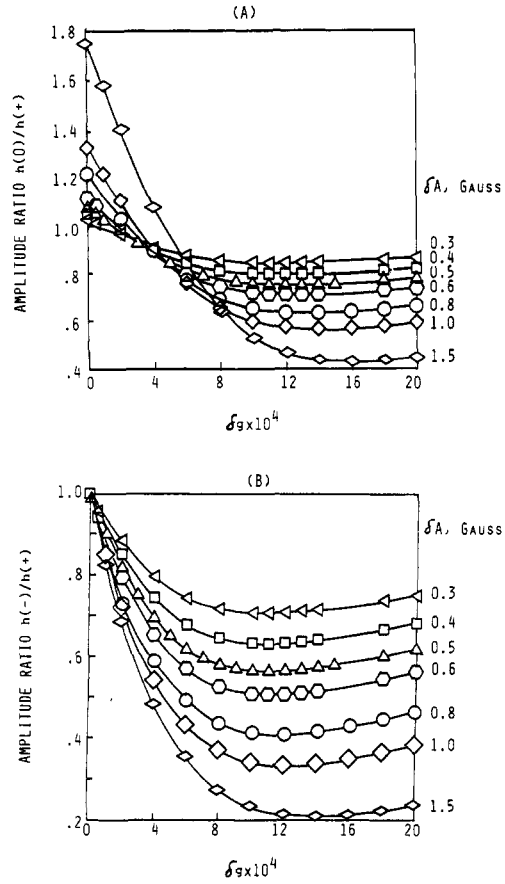

Figure 16. Variation of the amplitude ratios $r(0)$ and $r(-)$ in (A) and (B), respectively, as a function of δg values in the range of 0.0–0.0020 and δA in the range 0.3–1.5 G.

PCL.[15] This would create a more polar environment and would lead to an increase in A_{iso} and a decrease in g_{iso}. A distribution in these parameters would arise if the label samples a *range* of environments with different polarities; this is suggested by the experimental results. Additional proof that the environment of the spin label is different in IPNs and LBs compared to pure PVC is the observation of label decay in these samples above 415 K. This can be compared with the stability of the label in PVC up to at least 450 K.

It is also possible that the distributions observed in this study arise from the participation of the N–O groups of the label in hydrogen bonding.[43] Different strengths of the H bonds can also be expected in a polymer sample and their distribution is temperature dependent.[44] These phenomena can be translated into different local polarities and therefore different ESR parameters. The decrease in the effect on repeated heating at 400 K might be due to the breaking of the H bond and the isolation of the label in media of lower polarity. This suggestion is supported by the observation of separation of a PVC-rich phase in PVC/PCL blends on annealing at 373 K;[20] this effect has been detected by wide-angle X-ray scattering (WAXS).

The widths of the g_{iso} and A_{iso} distributions, δg and δA, are obviously related to the degree of compatibility, because in the limit of a single component, PVC, these distributions are equal to zero. Use of this argument for a more quantitative correlation between the distribution parameters and the morphology of the various blends will require very careful analysis of the line widths and examination of the changes in the line widths with the temperature and length of the annealing. These measurements are planned. Qualitatively, use of the distribution width as an indicator of mixing seems to lead to very logical conclusions. For instance, the LBs are more stable on annealing and the partition of the label in the polar and nonpolar environments is maintained. In contrast to these results, changes in the distribution widths of the IPNs on annealing might be due to kinetically controlled phase separation.

In some polymeric systems containing nitroxide probes, ESR line shapes similar to those reported in this study at 400 K have been detected.[45,46] In view of the approach described in this study, it is possible that the same interpretation can be applied.

In some cases ESR spectra that have the appearance of a superposition of *two* components can be simulated by assuming a single-site model, using, for instance, the "microscopic order–macroscopic disorder" (MOMD) model.[47] This model can be applied to systems with considerable local order; the polymers we have studied are not expected to qualify for this assumption. In addition, the line shapes predicted by this model do not seem to be in agreement with those presented here. This conclusion is reached when Figures 3 and 9 in ref 47 are compared with Figures 5–12 in this study. Moreover, in the high-temperature limit, this model does not predict the type of line shapes we have detected at 400 K.

The model VAR (very anisotropic reorientation)[47] also seems to predict single-site line shapes that appear similar to those normally interpreted in terms of two components. The line shapes predicted by this model are not in agreement with our results. In particular, a high-field signal appears to have a derivative shape (seen clearly in Figure 8 in ref 47), which is not observed in our ESR spectra.

Conclusions

ESR spectra from spin-labeled PVC indicate that the segmental motion around T_g is well described by the label

and the activation energy for this motion is 17.4 kcal/mol. It was found that T_{50G} is the same as T_g.

The spacial resolution of the label is of the order of 5–10 monomeric units of PVC. This means that the label is sensitive to the local structure in this range.

Polyurethane based on polycaprolactone glycol and MDI was spin labeled at the terminal isocyanate group; the ESR spectra show composite spectra, with fast and slow components.

Spin-labeled PVC was incorporated in semi-IPNs and in corresponding linear blends based on polyurethanes prepared from polycaprolactone glycol and MDI. Two components were detected in the ESR spectra from the IPNs and LBs. The lowest temperatures where an isotropic component was detected (for the fast components) and T_{50G} temperatures for the slow components are intermediate between the corresponding values in spin-labeled PU and the T_{50G} value for PVC.

We suggest that the two phases in PU consist of crystalline PCL and amorphous PCL; the aromatic isocyanates are part of the amorphous phase. The ESR results obtained for the IPNs and LBs suggest that PVC partitions between the two phases in PU.

The heterogeneity in the local environment of the label in IPNs and LBs is reflected in the line shapes detected around 400 K. These line shapes can be simulated by a distribution of ESR parameters such as g_{iso} and A_{iso} values. The existence of this distribution is supported by results from samples annealed at 400 K and by comparison of spectra from IPNs and LBs with those obtained for spin-labeled PVC. Qualitatively, the width of the distribution for each system, deduced from simulated spectra, is an indicator of the degree of mixing.

The distribution is thought to arise from a range of local environments of the label, differing in their polarity. Hydrogen bonding between the methine hydrogen in PVC to the carbonyl group in PCL and hydrogen bonding between the N–O group of the label and the N–H group of the urethane might increase the local polarity compared with that in pure PVC and give rise to the assumed distribution widths of δg and δA.

Acknowledgment. This study was supported by the Army Research Office through a Graduate Fellowship to R.D.H., by an NSF Instrumentation Grant for the acquisition of the ESR spectrometer, and by the University of Detroit computer center. We thank M. Omoto and J. Kusters for their help in the preparation of some samples and for numerous helpful discussions. We are grateful to a reviewer who encouraged us to examine our conclusions in view of the models described in ref 47.

References and Notes

(1) *Molecular Motion in Polymers by ESR*; Boyer, R. F., Keinath, S. E., Eds.; Harwood Academic: New York, 1980.
(2) Brown, I. M. *Macromolecules* **1980**, *14*, 801.
(3) Noel, C.; Laupretre, F.; Friedrich, C.; Leonard, C.; Halary, J. L.; Monnerie, L. *Macromolecules* **1986**, *19*, 201.
(4) Pekcan, O.; Kaptan, Y.; Demir, Y.; Winnik, M. A. *J. Colloid Interface Sci.* **1986**, *111*, 269.
(5) Kusumoto, N.; Sano, S.; Zaitsu, N.; Motozato, Y. *Polymer* **1976**, *17*, 448.
(6) Bullock, A. T.; Cameron, G. G.; Miles, I. S. *Polymer* **1982**, *23*, 1536.
(7) Theodorou, M.; Jasse, B. *J. Polym. Sci., Polym. Phys. Ed.* **1986**, *24*, 2643 and references therein.
(8) McCall, D. W. *Natl. Bur. Stand. Spec. Publ.* **1968**, *No. 301*, 475.
(9) Koleske, J. V.; Lundberg, R. O. *J. Polym. Sci., A* **1972**, *10*, 323.
(10) Phillips, P. J.; Rensch, G. J.; Taylor, K. D. *J. Polym. Sci., Polym. Phys. Ed.* **1987**, *25*, 1725.
(11) Brode, G. L.; Koleske, J. V. *J. Macromol. Sci. Chem.* **1972**, *A6*, 1109.
(12) Olabisi, O. *Macromolecules* **1975**, *8*, 316.
(13) Coleman, M. H.; Zarian, J. *J. Polym. Sci., Polym. Phys. Ed.* **1979**, *17*, 837.
(14) Albert, B.; Jerome, R.; Teyssie, P.; Smyth, G.; McBrierty, V. J. *Macromolecules* **1984**, *17*, 2552.
(15) Kintanar, A.; Jelinski, L. W.; Gancarz, I.; Koberstein, J. T. *Macromolecules* **1986**, *19*, 1876.
(16) Jones, M. G. B. M.; Hayward, D.; Pethrick, R. A. *Eur. Polym. J.* **1987**, *23*, 855.
(17) Leung, L. M.; Koberstein, J. T. *Macromolecules* **1986**, *19*, 706.
(18) Koberstein, J. T.; Gancarz, I.; Clarke, T. C. *J. Polym. Sci., Polym. Phys. Ed.* **1986**, *24*, 2487.
(19) Van Bogart, J. W. C.; Gibson, P. E.; Cooper, L. S. *J. Polym. Sci., Polym. Phys. Ed.* **1983**, *21*, 65.
(20) Shilov, V. V.; Blizhyuk, V. N.; Lipatov, Yu. S. *J. Mater. Sci.* **1987**, *22*, 1563.
(21) Hibino, K. M.Sc. Thesis, University of Detroit, 1985.
(22) Schlick, S.; Harvey, R. D.; Kusters, J.; Omoto, M.; Klempner, D. *Polym. Prepr. (Am. Chem., Soc. Polym. Div.)* **1987**, *28*, 167.
(23) Wang, C. L.; Klempner, D.; Frisch, K. C. *J. Appl. Polym. Sci.* **1986**, *32*, 4197.
(24) McCalley, R. C.; Shimshick, E. J.; McConnell, H. M. *Chem. Phys. Lett.* **1972**, *13*, 115.
(25) Goldman, S. A.; Bruno, G. V.; Freed, J. H. *J. Phys. Chem.* **1972**, *76*, 1858.
(26) Kuznetsov, A. N.; Ebert, B. *Chem. Phys. Lett.* **1974**, *25*, 342.
(27) Kivelson, D. *J. Chem. Phys.* **1960**, *33*, 1094.
(28) Rabold, G. P. *J. Polym. Sci., A* **1969**, *7*, 1203.
(29) Kumler, P. L.; Boyer, R. F. *Macromolecules* **1976**, *19*, 903.
(30) Kovarskii, A. L.; Wasserman, A. M.; Buchachenko, A. L., in ref 1, p 177.
(31) Hwang, J. S.; Saleem, M. M.; Tsonis, C. P. *Macromolecules* **1985**, *18*, 2051.
(32) Ferry, J. D. *Viscoelastic Properties of Polymers*; Wiley: New York, 1980; pp 486–496.
(33) Ward, T. C.; Books, J. T. *Macromolecules* **1974**, *7*, 207.
(34) Lembicz, F.; Slonecki, J.; Skolimowski, J. *Ser. Fiz. (Uniw. im. Adama Mickiewicza Poznaniu)* **1985**, *54*, 317.
(35) Shiotani, M.; Sohma, J.; Freed, J. H. *Macromolecules* **1983**, *16*, 1495.
(36) Froncisz, W.; Hyde, J. S. *J. Chem. Phys.* **1980**, *73*, 3123.
(37) Schlick, S.; Alonso-Amigo, M. G. *J. Chem. Soc., Faraday Trans. 1* **1987**, *83*, 3575.
(38) (a) Kasai, P. H. *J. Am. Chem. Soc.* **1972**, *94*, 5950. (b) Kasai, P. H. *J. Phys. Chem.* **1986**, *90*, 5034.
(39) *Spin Labeling; Theory and Applications*; Berliner, L. J., Ed.; Academic: New York, 1976; Vols. I–II.
(40) Morrisett, J. D., in ref 39, p 273.
(41) McConnell, H. M., in ref 39, p 527.
(42) Baglioni, P.; Ferroni, E.; Martini, G.; Ottaviani, M. F. *J. Phys. Chem.* **1984**, *88*, 5107.
(43) Wuu, S. K.; Kispert, L. D. *Fuel* **1985**, *64*, 1681.
(44) Coleman, M. M.; Lee, K. H.; Skrovanek, D. J.; Painter, P. C. *Macromolecules* **1986**, *19*, 2149
(45) Gupta, A.; Tsay, F. D. *J. Polym. Sci., Poly. Phys. Ed.* **1987**, *25*, 855.
(46) Hamada, K.; Iijima, T.; McGregor, R. *Macromolecules* **1986**, *19*, 1443.
(47) Meirovitch, E.; Nayeem, A.; Freed, J. H. *J. Phys. Chem.* **1984**, *88*, 3454.